Constitutive modelling of an arterial wall supported by microscopic measurements

J. Vychytil[a,*], P. Kochová[a], Z. Tonar[a], J. Kuncová[b], J. Švíglerová[b]

[a]*Faculty of Applied Sciences, University of West Bohemia in Pilsen, Univerzitní 22, 306 14 Pilsen, Czech Republic*
[b]*Faculty of Medicine in Pilsen, Charles University in Prague, Lidická 1, 301 66 Pilsen, Czech Republic*

Abstract

An idealized model of an arterial wall is proposed as a two-layer system. Distinct mechanical response of each layer is taken into account considering two types of strain energy functions in the hyperelasticity framework. The outer layer, considered as a fibre-reinforced composite, is modelled using the structural model of Holzapfel. The inner layer, on the other hand, is represented by a two-scale model mimicing smooth muscle tissue. For this model, material parameters such as shape, volume fraction and orientation of smooth muscle cells are determined using the microscopic measurements. The resulting model of an arterial ring is stretched axially and loaded with inner pressure to simulate the mechanical response of a porcine arterial segment during inflation and axial stretching. Good agreement of the model prediction with experimental data is promising for further progress.

1. Introduction

Mechanical response of an arterial wall is often predicted using hyperelastic models in the framework of continuum mechanics. In that case, the stress-strain relationship is defined via the so-called strain energy function representing the density of the Helmholtz free energy. In order to fit experimental data, phenomenological models such as the Mooney-Rivlin, the Ogden or the exponential model of the Fung's type are introduced using the empirical formulae of strain energy functions, see e.g. [3, 14]. Although widely used (see e.g. [1, 2, 18]), their application on the description of arterial wall is limited due to its complex microstructure. Phenomenological models may be suitable for the description of an overall mechanical response, however, they are incapable of providing the insight into the microscopic level. At the same time, physical meaning of the material constants appearing in these models is not always clear. The least-squares fitting instead of direct measurements must be applied for their identification, as it is detailed e.g. in [13].

Therefore, an increasing effort has been made in developing so-called structural models that are able to relate the overall mechanical response to the corresponding effects at microscopic level. An example of the strain energy function, proposed with respect to the underlying microstructure, is shown in [7] and [9]. In both cases, anisotropy and the structure of arterial layers are taken into account via a single parameter representing the angle between preferred fibre directions. The first mentioned model is later improved in [5] by considering the dispersion of fibres orientation. Possible application is shown in [6] for the soft tissue remodeling, i.e. the

---

*Corresponding author. Tel.: +420 377 632 390, e-mail: vychytil@kme.zcu.cz.

alignment of collagen fibres along the directions of principal stresses. In [10], an anisotropic hyperelastic model is proposed for fibre-reinforced materials. Taking into account an arbitrary number of fibre families, the strain energy function is proposed as a sum of exponential functions which makes it suitable for the description of soft collagenous tissues. Also, an issue of polyconvexity as a favourable property of strain energy functions is addressed. The model is generalized in [4] and applied for the description of uniaxial and biaxial tension tests with human coronary arteries and abdominal aorta. In this case, five material parameters are determined upon the comparison with experimental data.

Another approach of including the fibrous nature of the soft tissue into a hyperelastic model is demonstrated in [20]. Here the eight chain model is introduced as a representative volume element of the arterial layer. As a result, orthotropic strain energy function of the tissue is obtained respecting the entropy elasticity of individual polymer chains. Especially in this case of the bottom-up approach, all material parameters have a clear physical meaning related to the microstructure. However, as in the case of the angle between fibre orientation in [7], most of these parameters have to be determined by the least-squares fitting as their direct identification is not feasible.

The aim of this work is to contribute to the trend of the bottom-up approach in the constitutive modelling of arteries by employing the two-scale hyperelastic model which is based on the arrangement of soft tissues at the cellular level. The paper is organized as follows. In section 2 an idealized model of an artery is proposed as a two-layer thick walled tube composed of media and adventitia layers. Description of kinematics follows the approach proposed in [7] considering three configurations. Hence, residual stresses are taken into account via a parameter representing the opening angle of the arterial ring at the reference state. Distinct mechanical properties of individual layers are taken into account by considering two types of strain energy functions. Adventitia, the outer layer, is represented by the structural model of Holzapfel et al. proposed in [7]. Media, on the other hand, is described using the so-called "balls and springs" (BS) model introduced in [8].

Direct identification of some of the model parameters is done in section 3. Experimental methods of stereological assessment are performed for the smooth muscle tissue of a porcine abdominal aorta and a gastropod as it is detailed in [16, 17]. Thus the structural information is obtained, namely the relative volume fraction of smooth muscle cells within the media, their orientation, their size and their shape. It corresponds directly to several constants appearing in the BS model representing the material of media. Moreover, thickness of both media and adventitia is determined for a carotid artery from a freshly killed domestic pig.

Finally, the model predictions are compared to the experimental data in section 4. The porcine carotid artery is stretched longitudinally and pressurized at the same time following the experimental procedure described in [19]. As a result, pressure-diameter diagram is obtained for a given value of the axial stretch. Theoretical curves predicted by the model are obtained using the combination of both direct measurement of material parameters and the least-squares fitting.

2. Model of an arterial segment

2.1. Description of deformations

An arterial segment is considered as an axisymmetric thick-walled tube consisting of two layers, the media (inner) and the adventitia (outer). Its description follows the approach detailed in [7, 19]. The reference configuration is characterized with the length L, inner and outer radii
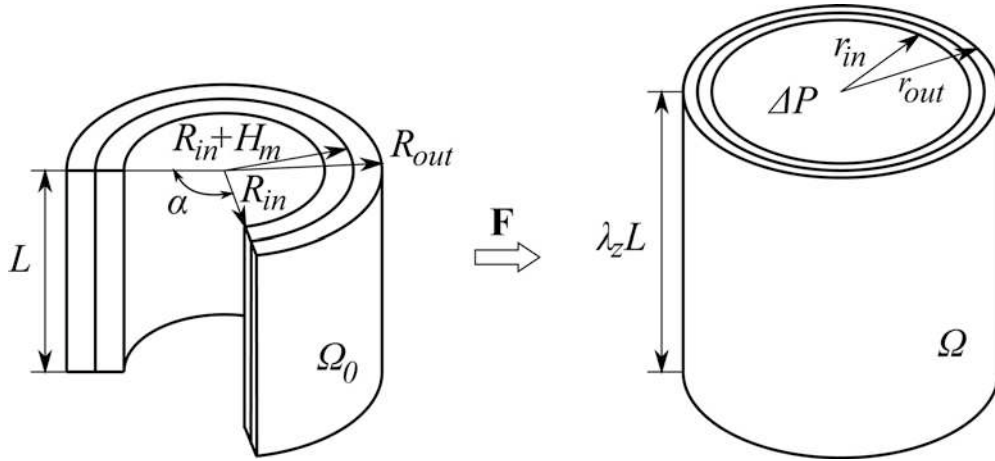
Fig. 1. The reference (left) and the current configuration (right) of an arterial segment loaded with inner pressure and axial stretch

R_{in}, R_{out}, media thickness H_m and the opening angle α, see Fig. 1. Loaded with the inner pressure ΔP and the axial stretch λ_z, the segment occupies the current configuration characterized with the length $\lambda_z L$, and the inner and outer radii r_{in}, r_{out}. Clearly, we assume the segment remaining as an axisymmetric tube also at this configuration, see Fig. 1. Due to the symmetry of the geometry and the loading, the description of kinematics is in fact reduced into a one-dimensional problem of the deformed radius $r(R)$. Applying the assumption of incompressibility, it is given with the formula

$$r(R) = \sqrt{\frac{R^2}{h\lambda_z} + C}. \tag{1}$$

Here, h is a parameter related to the opening angle as

$$h = \frac{2\pi}{2\pi - \alpha}, \tag{2}$$

quantifying in fact the residual stress and C is a constant to be determined from the boundary conditions. Applying the constitutive equations of hyperelasticity,

$$\boldsymbol{\sigma} = \frac{\partial \hat{W}}{\partial \mathbf{F}} \mathbf{F}^T - p\mathbf{I}, \tag{3}$$

we obtain the relationship between ΔP and C,

$$\Delta P = \int_{R_{in}}^{R_{in}+H_m} \frac{r'}{r} \left(\frac{hr}{R} \hat{W}_2^m - r' \hat{W}_1^m \right) \mathrm{d}R + \int_{R_{in}+H_m}^{R_{out}} \frac{r'}{r} \left(\frac{hr}{R} \hat{W}_2^a - r' \hat{W}_1^a \right) \mathrm{d}R. \tag{4}$$

Here, $\boldsymbol{\sigma}$ is the Cauchy stress tensor, $\hat{W}$ the strain-energy function, $\mathbf{F}$ the deformation gradient, p the hydrostatic pressure and the superscripts m and a refer to the media and adventitia, respectively. The notion $\hat{W}_i$ stands for the partial derivative of $\hat{W}$ with respect to the corresponding diagonal component of the deformation gradient,

$$\hat{W}_i = \frac{\partial \hat{W}}{\partial \lambda_i}, \quad \lambda_i = F_{ii}. \tag{5}$$

2.2. Material models

In agreement with [7], the adventitia is considered as a fibre-reinforced composite, characterized by the strain energy function

$$\hat{W}^a = \frac{\mu}{2}\left(\hat{I}_1 - 3\right) + \frac{\kappa_1}{2\kappa_2}\left[\left(e^{\kappa_2(\hat{I}_4-1)^2} - 1\right) + \left(e^{\kappa_2(\hat{I}_6-1)^2} - 1\right)\right], \tag{6}$$

where μ, κ_1 and κ_2 are material constants, $\hat{I}_1$, $\hat{I}_4$ and $\hat{I}_6$ are invariants and pseudo-invariants, respectively. They are defined as

$$\hat{I}_1 = \text{tr}\,\hat{\mathbf{C}}, \quad \hat{I}_4 = \hat{\mathbf{C}} : \mathbf{A_1}, \quad \hat{I}_6 = \hat{\mathbf{C}} : \mathbf{A_2}, \quad \mathbf{A_1} = \boldsymbol{a_{01}} \otimes \boldsymbol{a_{01}}, \quad \mathbf{A_2} = \boldsymbol{a_{02}} \otimes \boldsymbol{a_{02}}. \tag{7}$$

Here, $\hat{\mathbf{C}}$ is the distortional component of the right Cauchy-Green tensor,

$$\hat{\mathbf{C}} = (\det \mathbf{C})^{-1/3}\mathbf{C}, \qquad \mathbf{C} = \mathbf{F}^T\mathbf{F}. \tag{8}$$

The material is supposed to be reinforced by two families of fibres with predominant directions $\boldsymbol{a_{01}}$ and $\boldsymbol{a_{02}}$.

Note that the strain-energy function (6) is in fact composed of two contributions. The first one corresponds to the isotropic mechanical response of the matrix and is represented by the neo-Hookean term. The second one corresponds to the anisotropic mechanical response due to collagen fibres. The fibres are supposed to form a symmetrical structure so that their direction vectors can be expressed as

$$\boldsymbol{a_{01}} = [0, \cos\beta, \sin\beta]^T, \qquad \boldsymbol{a_{02}} = [0, \cos\beta, -\sin\beta]^T. \tag{9}$$

The angle β between the fibres represents an additional parameter appearing in the material model, see Fig. 2.

Media, on the other hand, is of different structure. Focusing on the contribution of the smooth muscle tissue we use the two-scale hyperelastic model introduced in [8]. Its microstructure is formed of incompressible balls interconnected mutually via linear springs to mimic the arrangement of smooth muscle cells and extracellular matrix. Each ball is also reinforced with
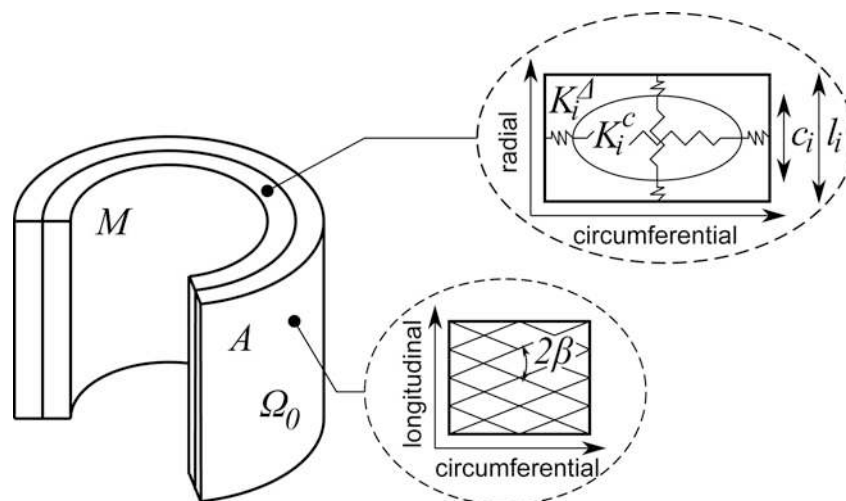

Fig. 2. Representative volume elements of the material models corresponding to the continuum points in the adventitia (A) and the media (M) layers. Two-dimensional sections are depicted for simplicity

linear springs representing cytoskeleton. Hence we call it the "balls and springs" (BS) model. The representative volume element (RVE) of the BS model is depicted in Fig. 2. Here, l_i denotes the sizes of the RVE, c_i the sizes of the ellipsoidal ball, K_i^c the stiffness of the springs reinforcing the ball and K_i^Δ the stiffness of the springs representing the extracellular matrix. The subscript i denotes the spatial direction, $i = 1, 2, 3$. The strain energy function can be expressed in the form

$$W^m = \sum_{\substack{i=1 \\ i \neq j \neq k}}^3 \frac{K_i}{2} \frac{k_i}{1+k_i} l_{ij} l_{ik} \left(\lambda_i - 1\right)^2 + \min_{\substack{r_i \\ r_1 r_2 r_3 = 1}} \sum_{\substack{i=1 \\ i \neq j \neq k}}^3 \frac{K_i}{2}(1+k_i)g_i^2 l_{ij} l_{ik} \left(r_i - \lambda_i^{eff}\right)^2. \quad (10)$$

Here, the effective stretches are introduced,

$$\lambda_i^{eff} = \frac{\lambda_i - 1}{g_i(1+k_i)} + 1. \quad (11)$$

The material parameters of this model are derived from the microscopic level as

$$K_i = \frac{K_i^\Delta}{l_i}, \qquad k_i = \frac{K_i^c}{K_i^\Delta}, \qquad l_{ij} = \frac{l_i}{l_j}, \qquad g_i = \frac{c_i}{l_i}. \quad (12)$$

Although the strain energy function is formed solely by quadratic contributions of the stretched/compressed springs connected in a simply-looking structure, the resulting formula (10) is rather complex. The reason for this is due to the configuration of inner structure represented by the shape of the ball. Instead of simply assuming the shape of the ball to be governed by the macroscopic deformation gradient (affine micro-deformations), it is "allowed" to occupy the shape which minimizes the overall deformation energy of the RVE. Hence, the strain energy function is split into a part describing an averaged spring elasticity of whole RVE and a part expressing the corresponding minimization problem. The dependence on the shape of the ball is given via dimensionless parameters r_i,

$$r_i = \frac{c_i'}{c_i}, \quad (13)$$

where c_i' represent sizes of the ball at the actual configuration. Clearly, the constraint

$$r_1 r_2 r_3 = 1, \quad (14)$$

stands for the incompressibily of the ball. Notice that the reference configuration of this model coincides with the natural one of zero strain energy as

$$r_i = 1, \qquad \lambda_i = 1 \Rightarrow \lambda_i^{eff} = 1, \qquad W^m = 0. \quad (15)$$

It means that there is neither tension nor compression within springs forming the RVE at the reference state and hence it is stress-free. Unfortunately, the minimization problem (10) has no analytical solution in general. Therefore, there is no analytical formula regarding stress-strain relationship which means that stress components have to be calculated numerically using the definition (3).

It is worth stressing that the proposed model is orthotropic and has a large number of material parameters. However, concerning the smooth muscle tissue within arterial wall, the assumption of the transverse isotropy is employed considering the radial and longitudinal directions to be equivalent. This assumption result in the total number of seven material parameters, namely K_1, K_2, k_1, k_2, g_1, g_2 and l_{12}.

3. Identification of model parameters

3.1. Geometry of an arterial ring and the media thickness

A sample of carotid artery was taken from a minipig involved in another experiment performed at the experimental facility of the Faculty of Medicine in Pilsen. The animal received humane care in compliance with the European Convention on Animal Care and the whole project was approved by the Faculty Committee for the Prevention of Cruelty to Animals. The carotid artery was rinsed with Tyrode's solution and placed in ice-cold Tyrode's solution. An approximately 1 cm-long ring was taken from the artery to assess its geometrical parameters, i.e. the inner and outer radii and the opening angle. Using three measurements at each end of the sample, the mean values were obtained as $R_{in} = 1.29$ mm, $R_{out} = 1.49$ mm and $\alpha = 108°$.

The sample was then fixed in 10 % formalin, dehydrated in graded ethanol solutions and embedded in paraffin blocks for histological analysis. The tissue block was cut transversally into 5 μm-thick histological sections, mounted on slides and stained with Verhoeff's haematoxylin and green trichrome [12] in order to show the overall layers of the arterial wall (the intima, the media, and the adventitia) and to distinguish elastin, collagen fibres, and vascular smooth muscle cells (SMC). The cytoplasm of SMC stains reddish with the acid fuchsin. Four micrographs were analyzed using the Ellipse software (ViDiTo, Košice, Slovakia). They were sampled in a systematic uniform random manner round the circumference of the carotid wall. The intima-media thickness was measured using a line tool connecting the surface of the intima with the most external layer of the compact vascular smooth muscle of the media, see Fig. 3. As the intima was represented only by a single layer of endothelium supported with a very thin layer of subendothelial connective tissue, it was neglected in agreement with model assumptions. The measurements thus resulted in a mean value of media thickness, $H_m = 0.89$ mm.
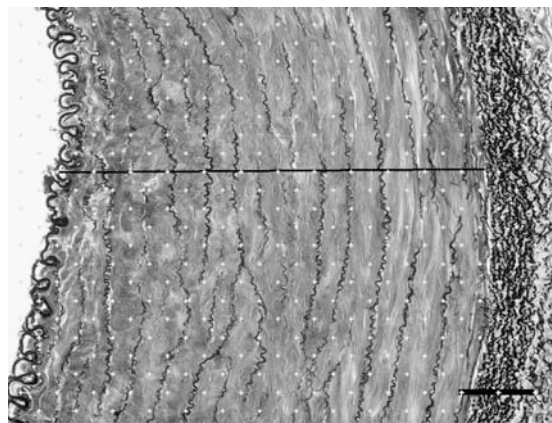

Fig. 3. The intima media thickness (black line) was measured three times per micrograph. Modified green trichrome stain, scale bar 100 μm

3.2. Orientation of smooth muscle tissue within media

Unlike the contours of individual muscle cells, the nuclei are easy to be visualized in routine histological sections. As the smooth muscle cells are spindle shaped and the long axes of their oval nuclei run parallel to the long axis of the muscle cells, describing the orientation of the nuclei is a good estimate for assessing the orientation of the whole smooth muscle cells. For the model presented in this paper, we use the previously published distribution of angles between
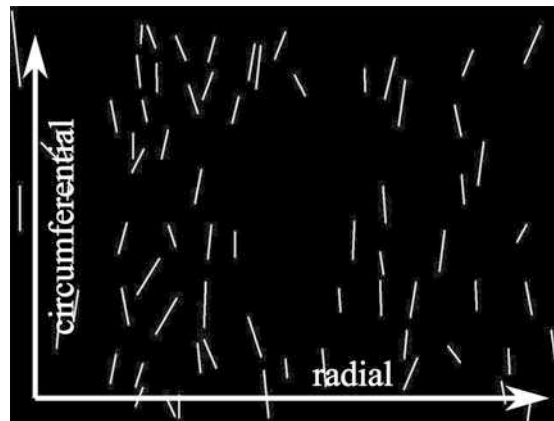
Fig. 4. Orientation of nuclei of smooth muscle cells in a transverse section of tunica media of porcine aorta. Based on a method previously published in [17]

the long axes of smooth muscle cells and the circumferential direction of arterial wall [17]. In the transverse section, the angle ranges within the interval $\langle -38; 35 \rangle^\circ$, i.e. the orientation of nuclei and therefore smooth muscle cells is considered as circumferential, see Fig. 4.

3.3. Model parameters of a single smooth muscle cell

Due to the variability in size and shape of individual biological cells, estimating of their typical morphological parameters relies on stochastic geometry. Morphometric characteristics of vascular smooth muscle cells have not been published so far, therefore we use the values published in gastropod smooth muscle cells, where the mean cell volume is $1\,358\ \mu\mathrm{m}^3$ [11, 16] and the maximum transversal diameter is approx. $6\ \mu$m [15]. If the shape of smooth muscle cell is approximated by an ellipsoid with the minor axes of the same size, its length is calculated as $72\ \mu$m.

Concerning the proposed model, the observed orientation of smooth muscle tissue and the parameters of individual cells result in following conclusions. First, the model is considered as transversally isotropic with the sizes of the ball $c_1 = c_3 = 6\ \mu$m, $c_2 = 72\ \mu$m. Second, the main axes of the ball and therefore the orientation of the RVE correspond to the spatial directions of the cylindrical coordinate system as it is depicted in Fig. 2.

3.4. Volume fraction of smooth muscle cells

In order to determine the relative size of the ball within the RVE in our model, the volume fraction of smooth muscle cells is employed. This parameter represents the ratio of the volume of cells and the volume of the whole tunica media. We use the values for the porcine abdominal aorta published in [17]. Here the stereological point-grid method is used, allowing a reliable estimation of area fraction of smooth muscle cells within the media. According to the Cavalieri principle, the volume fraction is estimated with the mean value of $V_{rel} = 0.65$.

In the BS model, let us assume the thickness of the extracellular matrix is expressed with a constant δ in all three spatial directions, i.e.

$$l_i = c_i + \delta. \tag{16}$$

Introducing the dimensionless parameters $\delta^* = \delta/c_1$ and $c^* = c_2/c_1 = 12$, the expression for

the relative volume fraction,

$$V_{rel} = \frac{c_1^2 c_2}{l_1^2 l_2},$$

(17)

leads to the equation

$$(\delta^*)^3 + (2 + c^*)(\delta^*)^2 + (2c^* + 1)\delta^* + \left(1 - \frac{1}{V_{rel}}\right)c^* = 0.$$

(18)

As a solution of this equation, parameter δ^* is obtained. Finally, using the definitions (12) and (16), three material parameters of the BS model are identified,

$$g_1 = \frac{1}{1 + \delta^*} \doteq 0.81, \qquad g_2 = \frac{c^*}{c^* + \delta^*} \doteq 0.98, \qquad l_{12} = \frac{1 + \delta^*}{c^* + \delta^*} \doteq 0.10.$$

(19)

4. Mechanical response of an arterial segment during inflation and axial stretching

4.1. Experimental data

In order to compare the model predictions with experimental data, a sample of porcine carotid artery is investigated. Namely, we use the sample described in section 3.1. The experiment follows the procedure that is detailed in [19]. Therefore, only a brief summary is given in this section. The sample is clamped into a measurement device (Tissue bath MAYFLOWER, Perfusion of tubular organs version, type 813/6, Hugo Sachs Electronik, Germany) with the axial stretch of $\lambda_z = 1.5$ to mimic *in vivo* conditions. After preconditioning, the sample is loaded with inner pressure from 0 up to 200 mm Hg. At the same time the outer diameter is measured at the middle region of the segment. Resulting pressure-diameter diagram is plotted in Fig. 5. Here the units are converted as 1 mm Hg = 133.322 Pa.

4.2. Model predictions

Theoretical pressure-diameter curves are obtained by the model of an arterial segment using the formulae derived in section 2 and the material parameters obtained in section 3. As an axisymmetric tube formed of two layers, its geometry is described with inner radius $R_{in} =$
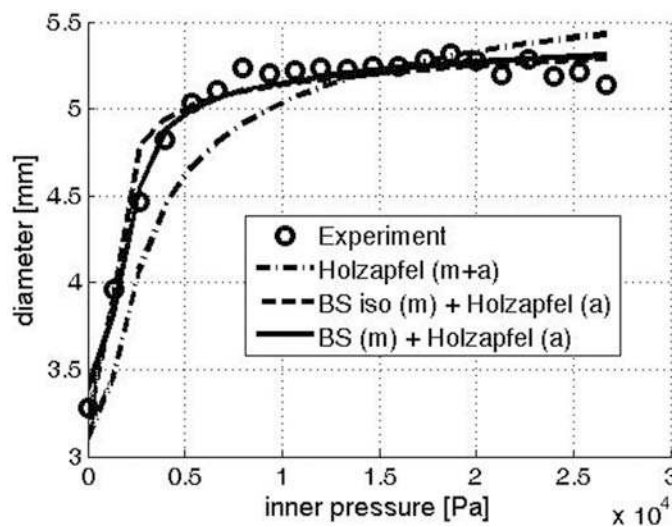

Fig. 5. Experimental pressure-diameter diagram and the theoretical curves

1.29 mm, outer radius $R_{out} = 2.49$ mm, opening angle $\alpha = 108°$ and the media thickness $H_m = 0.89$ mm. Adventitia, the outer layer, is considered as the structural material model of Holzapfel with four unknown material parameters, μ, κ_1, κ_2, β. Concerning the media, described using the BS model, three material parameters related to the microstructure of smooth muscle tissue are determined by the microscopic measurements, namely $g_1 = 0.81$, $g_2 = 0.98$ and $l_{12} = 0.10$. However, four material parameters related to the stiffness of smooth muscle cells and extracellular matrix are unknown, i.e. K_1, K_2, k_1 and k_2. All the unknown parameters (eight in total) are obtained by the comparison of the theoretical pressure-diameter curve with the experimental data using the least-squares fitting. The result is plotted using the solid line in Fig. 5. Material parameters, obtained by the least-squares fitting, are listed in Table 1.

For comparison, two other models are considered. In the first one the isotropic restriction of the BS model is considered for media (dashed line). It corresponds to the cubic shape of the representative volume element containig spherical ball with stifnesses that are identical in all three spatial directions, i.e. $K_i^\Delta = K^\Delta$, $K_i^c = K^c$, $c_i = c$, $l_i = l$, see Fig. 2. Number of material parameters is thus reduced to three for this model, namely $K = K^\Delta/l$, $k = K^c/K^\Delta$, $g = c/l$. The structural parameter is identified using the volume fraction of smooth muscle cells as $g = \sqrt[3]{V_{rel}} \doteq 0.87$. The rest of the material parameters (six in total) is left for the least-squares fitting.

Table 1. The list of material parameters identified by the least-squares fitting

BS (m) + Holzapfel (a)	BS isotropic (m) + Holzapfel (a)	Holzapfel (m+a)
$K_1 = 5.9 \times 10^5$ Pa	$K = 5.9 \times 10^5$ Pa	$\mu^m = 1.8$ kPa
$K_2 = 5.9 \times 10^5$ Pa	$k = 9.8 \times 10^{-3}$	$\kappa_1^m = 1.1$ kPa
$k_1 = 1.8 \times 10^{-2}$		$\kappa_2^m = 0.2$
$k_2 = 2.1 \times 10^{-4}$		$\beta^m = 42°$
$\mu = 82$ Pa	$\mu = 66$ Pa	$\mu^a = 1.3 \times 10^2$ Pa
$\kappa_1 = 1.4 \times 10^2$ Pa	$\kappa_1 = 1.3 \times 10^2$ Pa	$\kappa_1^a = 1.8 \times 10^2$ Pa
$\kappa_2 = 2.2$	$\kappa_2 = 2.4$	$\kappa_2 = 1.5$
$\beta = 2.4°$	$\beta = 18°$	$\beta^m = 26°$

In the second case, the structural material model of Holzapfel is considered for both media and adventitia (dash-dotted line). In fact, it corresponds to the description of arterial wall as it is proposed in [7]. All material parameters (eight in total) must be determined by the least-squares fitting, namely μ^m, κ_1^m, κ_2^m, β^m, μ^a, κ_1^a, κ_2^a, β^a. Here the superscripts m and a refer to the media and the adventitia, respectively.

In all three models, good agreement with experimental data is provided. However, combination of the BS model with the model of Holzapfel seems to be more accurate in comparison to the case when the model of Holzapfel is considered for both media and adventitia. Concerning the material parameters related to the Holzapfel model, the values obtained by the least squares fitting are comparable to those considered for the rabbit carotid artery in [7]. Obviously, there is only a slight difference in the mechanical response of the BS model and its isotropic restriction. This is caused by the influence of adventitia which dominates the mechanical response for higher pressure (due to the exponential character of the model).

5. Conclusion

In this paper, an idealized model of an arterial segment as an axisymmetric tube is proposed. Although real arteries are composed of three layers, intima (the innermost layer) is very thin and makes an insignificant contribution to the overall mechanical response in healthy young arteries. Hence, it is neglected in this model.

Static analysis and description of deformations for the given load (axial stretch and inner pressure) follow the approach detailed in [7]. Due to the symmetry of the loading, the arterial segment keeps the shape of an axisymmetric tube also at the current configuration. During the experiment, on the other hand, the sample is clamped within the device and perfused intraluminarly which results in a more complex shape at the current configuration. However, accuracy of this simplification for the presented experimental setting is confirmed by FE analysis in [19].

Structural model of Holzapfel et al., employed for the description of the mechanical response of adventitia, is characterized with three material parameters related to stiffness and one material parameter related to structure. Although having a transparent physical meaning (angle between preferred fibre directions), direct identification of this parameter has not been done so far. Hence, the least-squares fitting is applied for all material parameters related to adventitia. BS model, representing the material of media, is proposed using the bottom-up approach which leads to the transparent physical meaning of all material parameters. Although this model is orthotropic in general, we use the transverse isotropic restriction upon the fact that smooth muscle cells are of approximately ellipsoidal shape with equal minor axes. Resulting material model is characterized with seven material parameters, three of them are identified directly using the microscopic measurements. It is worth stressing that the measurements take place using also the samples of porcine aorta and the smooth muscle tissue of gastropod even if the model represents an arterial segment of porcine carotid artery. Nevertheless, we assume this inconsistency to be tolerable for the particular parameters (relative volume fraction of smooth muscle cells in porcine aorta and shape of smooth muscle cells in gastropod). Performing these measurements in one sample corresponding to the model is favourable in future work though.

Comparison of the model prediction with the mechanical response of real arterial segment is performed using the porcine carotid artery undergoing inflation test. Theoretical curves exhibit a good agreement with experimental data, however, there are still eight material parameters identified by the least-squares fitting (six material parameters in the case of isotropic restriction). In the case of BS model, the resulting material parameters are of the order $K_i \sim 10^5$ Pa, $k_i \sim 10^{-4} \div 10^{-2}$, meaning the living cells to be much softer compared to the extracellular matrix within smooth muscle tissue. Concerning the Holzapfel model, the resulting material parameters are comparable and of the same order as the parameters published for rabbit carotid artery in [7]. Only the value of the angle β is scattered, however, there is no measurement so far which could be useful in identifying this structural parameter. Moreover, the existence of preferred fibre directions of collagen fibres within adventitia is questionable.

Difference in the mechanical response of the presented model and its isotropic restriction is of small significance namely for higher pressures. This is caused by the exponential character of the mechanical response of adventitia which dominates in the overall mechanical response and acts as a stiff tube reinforcing the arterial segment. This phenomena is in agreement with experimental observations, although undesirable in our research. To be able to study the effect of material parameters related to microscopic level on the overall mechanical response, loading of the media alone is preferable.

Another goal for future studies is to increase the number of material parameters identified directly and not using the least-squares fitting. Also, the presented material model of media is a very drastic simplification of real soft tissue. Improvement of this model using for instance polymer chains instead of linear springs or embedding motor proteins might help in studying some effects related to microscopic level such as prestress or smooth muscle tissue activation.

Acknowledgements

References

[1] Bathe, M., A fluid-structure interaction finite element analysis of pulsatile blood flow through a compliant stenotic artery, Bachelor thesis, MIT, 1998.

[2] Delfino, A., Stergiopulos, N., Moore, J. E., Meister, J.-J., Residual strain effects on the stress field in a thick wall finite element model of the human carotid bifurcation, Journal of Biomechanics 30(8) (1997) 777–786.

[3] Chuong, C. J., Fung, Y. C., Three-dimensional stress distribution in arteries, Journal of Biomechanical Engineering 105 (1983) 268–274.

[4] Ehret, A. E., Itskov, M., A polyconvex hyperelastic model for fiber-reinforced materials in application to soft tissues, Journal of Materials Science 42 (2007) 8 853–8 863.

[5] Gasser, T. C., Ogden, R. W., Holzapfel, G. A., Hyperelastic modelling of arterial layers with distributed collagen fibre orientation, Journal of the Royal Society Interface 3 (2006) 15–35.

[6] Hariton, I., deBotton, G., Gasser, T. C., Holzapfel, G. A., Stress-driven collagen fiber remodeling in arterial walls, Biomechanics and Modeling in Mechanobiology 6 (2007) 163–175.

[7] Holzapfel, G. A., Gasser, T. C., Ogden, R. W., A new constitutive framework for arterial wall mechanics and a comparative study of material models, Journal of Elasticity 61 (2000) 1–48.

[8] Holeček, M., Moravec, F., Hyperelastic model of a material which microstructure is formed of "balls and springs", International Journal of Solids and Structures 43 (2006) 7 393–7 406.

[9] Horny, L., Zitny, R., Chlup, H., Strain energy function for arterial walls based on limiting fiber extensibility, IFMBE Proceedings 22 (2008) 1 910–1 913.

[10] Itskov, M., Ehret, A. E., Mavrilas, D., A polyconvex anisotropic strain-energy function for soft collagenous tissues, Biomechanics and Modeling in Mechanobiology 5 (2006) 17–26.

[11] Kochova, P., Study of mechanical properties of smooth muscle tissue from cellular level, Ph.D thesis, University of West Bohemia in Pilsen, 2008.

[12] Kočová, J., Overall staining of connective tissue and the muscular layer of vessels. Folia Morphologica 18 (1970) 293–295.

[13] Lally, C., Reid, A. J., Prendergast, P. J., Elastic behavior of porcine coronary artery tissue under uniaxial and equibiaxial tension, Annals of Biomedical Engineering, 32 (10) (2004) 1 355–1 364.

[14] Ogden, R. W., Non-linear elastic deformations, Dover Publications, New York, 1997.

[15] Tonar, Z., Markoš, A., Microscopy and morphometry of integument of the foot of pulmonate gastropods Arion rufus and Helix pomatia. Acta veterinaria Brno 73 (2004) 3–8.

[16] Tonar, Z., Kochová, P., Holeček, M., Janáček, J., Stereological assessment, mechanical measurement and computer modelling of smooth muscle, Materials Science Forum 567–568 (2007) 353–356.

[17] Tonar, Z., Kochová, P., Janáček, J., Orientation, anisotropy, clustering, and volume fraction of smooth muscle cells within the wall of porcine abdominal aorta, Applied and Computational Mechanics 2 (2008) 145–156.

[18] Valencia, A., Solis, F., Blood flow dynamics and arterial wall interaction in a saccular aneurysm model of the basilar artery, Computers and Structures 84 (2006) 1 326–1 337.

[19] Vychytil, J., Moravec, F., Kochová, P., Kuncová, J., Švíglerová, J., Modelling of the mechanical behaviour of the porcine carotid artery undergoing inflation-deflation test, Applied and Computational Mechanics 4 (2010) 251–262.

[20] Zhang, Y., Dunn, M. L., Drexler, E. S., McCowan, C. N., Slifka, A. J., Ivy, D. D., Shandas, R., A microstructural hyperelastic model of pulmonary arteries under normo- and hypertensive conditions, Annals of Biomedical Engineering 33 (8) (2005) 1 042–1 052.